Supplementary Information

Electrochemically-driven drug metabolism via CYP1A2/ UGT1A10 bienzymes confined in graphene nano-cage

*Jusheng Lu, Yuanjian Zhang, Henan Li, Jiachao Yu and Songqin Liu**

Jiangsu Province Hi-Tech Key Laboratory for Bio-medical Research, School of Chemistry and Chemical Engineering, Southeast University, Nanjing 211189, China.

Reagents

Cytochrome P450 1A2 (CYP1A2) isozyme, UDP-glucuronic acid (UDPGA), alamethicin, chitosan were obtained from Sigma–Aldrich Co. Ltd. (St. Louis, MO, USA). Racemic warfarin was obtained from Toronto research chemicals Inc. (TRC, North York, Canada). UDP-glucuronosyltransferase 1A10 enzyme (UGT1A10) was obtained from Becton Dickinson Co. (Franklin Lakes, NT, USA).α-amino-ω-hydroxyl poly (ethylene glycol) (NH_2-PEG-OH, M_w=550, 1000 or 2000) was purchased from Shanghai Seebio Biotechnology Inc. (Shanghai, China). Graphite oxide was obtained from Nanjing XFNANO Materials Tech Co. (Nanjing, China).

Apparatus

Fourier transform infrared spectroscopy (FT-IR) was collected on a Tensor 27 instrument (Bruker Co. Ltd., Germany) using KBr pellets. UV-vis absorption spectra were measured on a UV-2450 spectrometer (Shimadzu, Japan). Raman spectra were collected with a DXR Raman microscope (Thermo Fisher Scientific Inc., USA) with an excitation wavelength of 532 nm. Transmission electron microscopy (TEM) and high resolution transmission electron

microscopy (HRTEM) were performed on a JEM-2100 transmission electron microscope (JEOL, Japan) at an acceleration voltage of 200 kV.

Electrochemical measurements were performed on a CHI 750C electrochemical workstation (Shanghai Chenhua Co. Ltd., China) with a conventional three-electrode system of a modified glassy carbon electrode (GCE, Φ3 mm) as the working electrode, a saturated calomel electrode (SCE) as the reference and a platinum wire electrode as the counter electrode, respectively.

Liquid chromatography-tandem mass spectrometry (LC-MS/MS) analyses for electrochemically driven drug metabolites of warfarin were performed using an Agilent series 1200 HPLC system, which was interfaced with Agilent Triple Quadrupole mass spectrometer (Agilent, Palo Alto, CA, USA). 5 μL of sample was injected into a 2.1 mm × 150 mm Zorbax Eclipse 5 μm XDB-C18 reverse-phase column. Mobile phases were 0.1% acetic acid and 5% acetonitrile in water (A) and 0.1% acetic acid in methanol (B). The flow rate was 0.6 mL min^{-1}. Compounds of interest were eluted using the following gradient: 100% A for the first 1.0 min, followed by a linear gradient from 100% to 5% A (1.0-10.0 min), 5% A and 95% B maintained for 2.0 min, and 5% to 100% A (12.0-12.5 min) with 100% A maintained 2.5 min. The total run time per sample was 15 min. All MS/MS analyses were performed in positive ion mode with ion spray voltage 5.5 kV, turbo heater temperature was 500 ^{o}C, curtain, nebulizer, turbo, and collisionally activated dissociation gases were 40, 50, 60, and 6 psi, respectively.

Synthesis of graphene-chitosan nanosheets (GR/CS).

Graphene oxide (GO) was obtained by exfoliation of graphite oxide under ultrasonication in a water bath for 2 h.[S1] The obtained brown dispersion was centrifuged at 3000 rpm for 30 min to remove any unexfoliated graphite oxide. Dialysis was performed to completely remove any residual salts. Then, 10 mL of the as-prepared GO (1.0 mg mL^{-1}) dispersion was mixed with 1 mL of 0.1 wt% CS in 1.0 wt% acetic acid solution. The obtained homogeneous GO/CS

nanocomposites were then stirred at 60 °C for 2 h. After that, 0.5 mL of 1.0 mM ascorbic acid was added and adjusted pH to 8.5 with 25 wt% ammonia solution, followed by continuous stirring at 95 °C for 15 min. The dispersion was then centrifuged, washed with water and dried in air for 24 h.

Covalent immobilization of CYP1A2 and UGT1A10 on the GR/CS nanosheets.

NH_2-PEG-C≡CH and NH_2-PEG-N_3 were synthesized according to the previous reports with slight modifications.[S2] The immobilization process of CYP1A2 and UGT1A10 was as follows:

(1) Covalent co-immobilization of CYP1A2 and NH_2-PEG-N_3 on the GR/CS. GCE was carefully polished to a mirror-like surface with 1.0, 0.3 and 0.05 μm alumina slurries, followed by rinsing thoroughly with water. After successive ultrasonication in ethanol and water for 3 min, respectively, the electrode was rinsed with water and dried under nitrogen stream. As shown in Fig. 1, 5.0 μL of 0.5 mg mL^{-1} GR/CS dispersion was dropped on the surface of the freshly pretreated GCE and dried in ambient air. Then the modified electrode was incubated with 20.0 μL of 1.0 wt% glutaradehyde solution in 0.1 M pH 7.4 PBS at room temperature for 2 h. After rinsing with water, the resultant GCE was immersed in 20.0 μL of the mixture solution containing CYP1A2 and NH_2-PEG-N_3 at 4 °C overnight with mild stirring. Subsequently, the electrode was rinsed with water to remove any nonspecific bound CYP1A2 and NH_2-PEG-N_3. The co-immobilization of CYP1A2 and NH_2-PEG-N_3 on GR/CS was thus achieved (denoted as GCE/GR/CS(CYP1A2) -PEG-N_3).

(2) Covalent co-immobilization of UGT1A10 and NH_2-PEG-C≡CH on GR/CS. 50.0 μL of 0.5 mg mL^{-1} GR/CS solution was mixed with 5.0 μL of 1.0 wt% glutaradehyde solution and incubated at room temperature for 2 h with stirring, follow by centrifuging, washing, and re-dispersing in 50.0 μL of 0.1 M pH 7.4 PBS. Subsequently, 50.0 μL of the mixture solution containing UGT1A10 and NH_2-PEG-C≡CH was added into the as-prepared glutaradehyde modified GR/CS suspension and incubated sequentially at 4 °C overnight with stirring. After

centrifugation and washing, the obtained UGT1A10 and NH_2-PEG-C≡CH modified GR/CS (denoted as GR/CS(UGT1A10)-PEG-C≡CH) was redispersed in 50.0 μL of PBS (pH 7.4).

Construction of CYP1A2/UGT1A10 bienzyme complexess in graphene nano-cage via a click reaction.

The construction of CYP1A2/YGT1A10 in graphene nano-cage was achieved by immersing the GR/CS(CYP1A2)-PEG-N_3 modified GCE in the GR/CS(UGT1A10) -PEG-C≡CH solution containing 1.0 mM copper (II) sulfate pentahydrate and 10 mM sodium ascorbate at 4 ^oC for 24 h in the dark under nitrogen atmosphere, and then, the electrode was rinsed with water and stored at 4 ^oC when not used.

Scheme S1

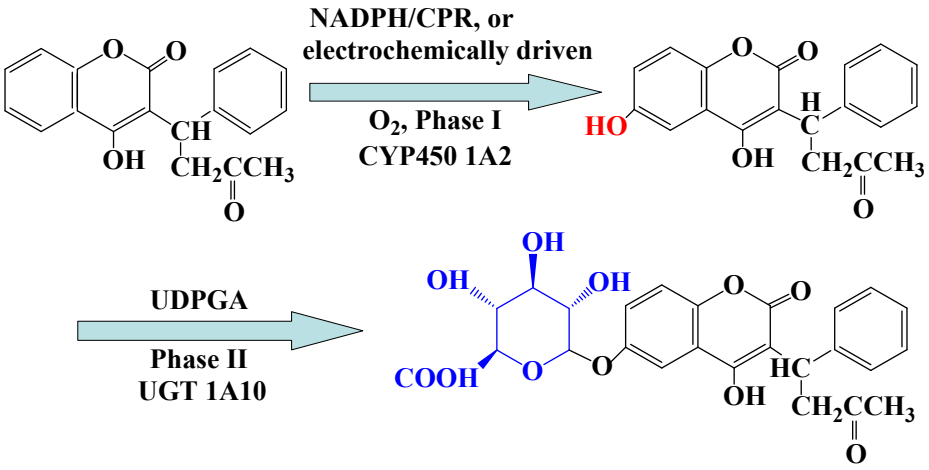

Scheme S1 Metabolic process of warfarin with NADPH or electrode as electron donor.

CPR stands for cyt P450 reductase, which is responsible for electron delivery from the NADPH to the heme center of CYP450.

Fig. S1

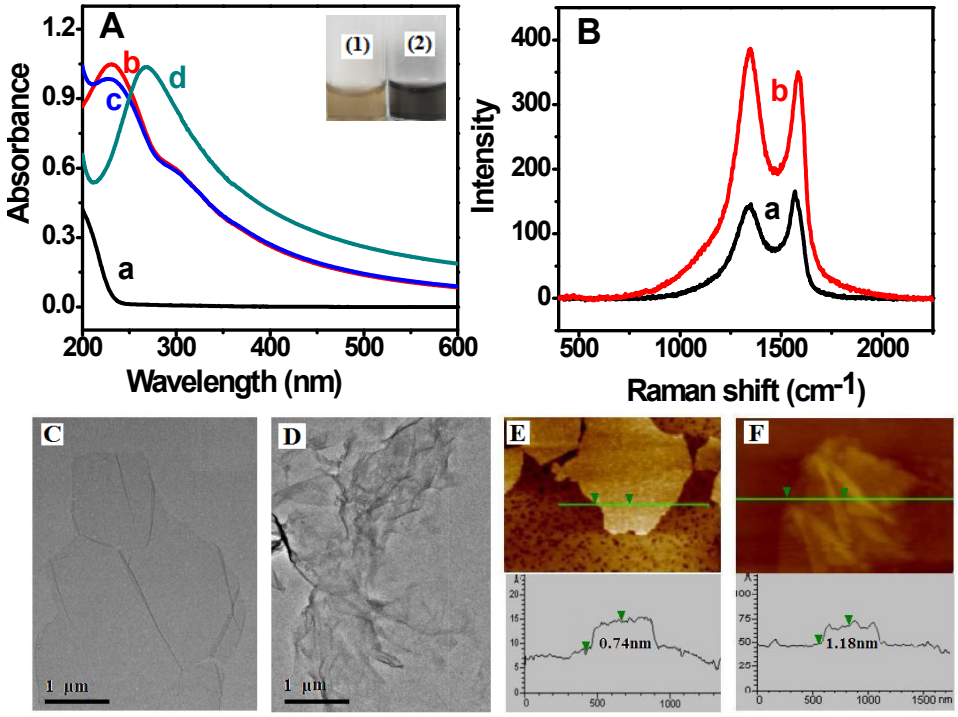

Fig. S1 Characterization of GR/CS. (A) UV-vis spectra of chitosan (a), GO (b), GO/CS (c) and GR/CS (d); inset: photos of GO/CS (1) and GR/CS (2) dispersion solution; (B) Raman spectra of GO (a) and GR/CS (b). TEM images of GO (C) and GR/CS (D). AFM images of GO sheet (E) and GR/CS (F) with height profiles.

Due to the abundant reactive hydroxyl and amino functional groups of CS, the oxygen containing groups and negative charges on the GO surface result in strong interactions between GO and the CS matrix through hydrogen bonding and electrostatic attraction.[S3] In the present work, GO was mixed first with CS to form a yellow-brown homogeneous solution (photo 1 in Fig. S1A). After it was reduced with ascorbic acid in an alkaline solution, the product could re-disperse into aqueous solution to form stable and homogeneous graphene-chitosan (GR/CS) dispersion due to the great amount of polar groups in the GR/CS nanosheets (photo 2 in Fig. S1A). Furthermore, the primary amine of the GR/CS nanosheets could be used to link the enzymes and amino terminated PEG covalently for the subsequent covalent construction of enzyme complexes in graphene nano-cage. UV-vis spectra, Raman

spectra, TEM and AFM measurements were used to characterize the GR/CS nanosheet (Fig. S1 A to F). The UV-vis spectra of GO and GO/CS (curves b and c in Fig. S1A) display two distinct absorption peaks. The one peak at 230 nm corresponds to the π-π* transitions of aromatic C–C bonds, and a shoulder around 304 nm can be assigned to n-π* transitions of C=O bonds on basal plane of GO. The absorption peak of GO at 230 nm red-shifts to 268 nm in GR/CS (curve d in Fig. S1A) after being further reduced by ascorbic acid, which indicates the restoration of the electronic conjugation within the graphene sheets.[S4] Disappearance of the absorption peak at 304 nm in GR/CS indicates the successful removal of the carbonyl group on GO through reduction.[S5] The Raman spectra (Fig. S1B) show that GO (curve a) has the characteristic peaks at 1568 cm^{-1} and at 1350 cm^{-1} corresponding to the G and the D bands of the graphene structure, respectively. GR/CS nanosheet (curve b in Fig. S1B) exhibits a similar Raman spectrum as GO indicating that the main graphene structure has been retained in the composite. The intensity ratio of D to G peak (I_D/I_G), known as Tuinstra–Koenig (TK) relation, is found to change inversely with graphitic domain size and widely used to study the crystalline quality of graphite or graphene after different kinds of treatment,[S6] from 0.88 to 1.10 indicating a decrease in the average size of the sp^2 domains upon reduction and combination with chitosan.[S7] TEM images clearly illustrate that GO (Fig. S1C) is a transparent ultra-thin flat sheet, while GR/CS (Fig. S1D) is translucent thin wrinkle film. Furthermore, AFM studies indicate that the GO sheet is single-layer with a mean thickness of 0.74 nm (Fig. S1E), while that of GR/CS is 1.18 nm (Fig. S1F), consistent with the thickness range (0.34-1.2 nm) of the single-layer graphene structure reported in the literatures.[S8] All these characterization results suggest that GR has combined successfully with CS and formed a single-layer nanosheet.

Fig. S2

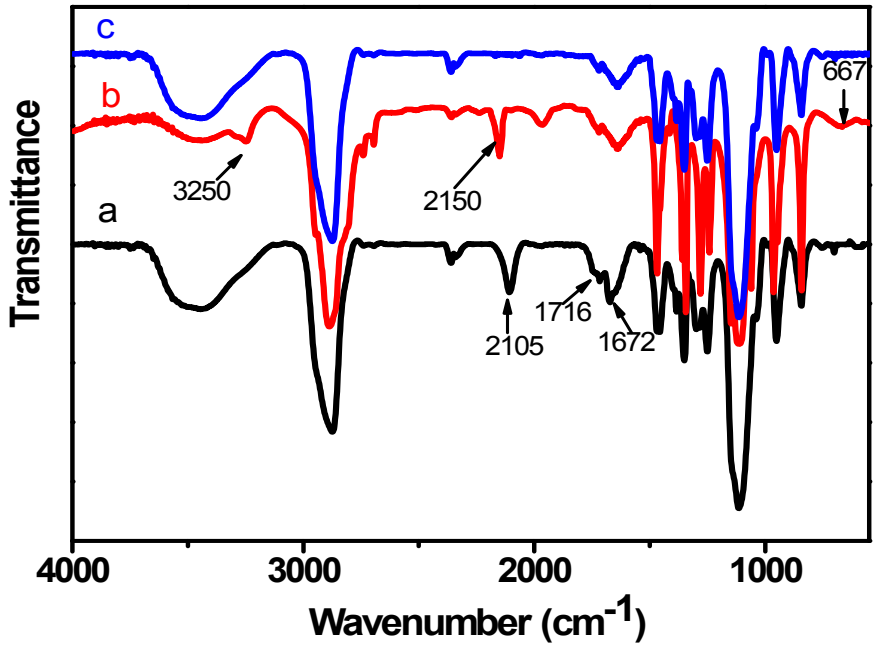

Fig. S2 FT-IR spectra. (a) GR/CS(CYP1A2)-PEG-N_3 (**1**); (b) GR/CS(UGT1A10)-PEG-C≡CH (**2**); (c) GR/CS(CYP1A2)-PEG-triazole-PEG-(UGT1A10) CS/GR (**3**).

In the presence of Cu(II), GR/CS(CYP1A2)-PEG-N_3 on the surface of GCE and GR/CS(UGT1A10)-PEG-C≡CH in the solution could be cross-linked by the sodium ascorbate induced click reaction between azide and alkyne under nitrogen atmosphere, thereby resulting in the covalent formation of the graphene nano-cage with 1,3-dipolar cycloaddition. The click chemistry reaction could be verified by FT-IR spectra (Fig. S2). The FT-IR spectrum of GR/CS(CYP1A2)-PEG-N_3 (curve a) showed a azide stretching absorption peak at 2105 cm^{-1}, and the -C≡CH characteristic infrared absorption peaks ($\upsilon_{\equiv C-H}$ 3250 cm^{-1}, $\upsilon_{C\equiv C}$ 2150 cm^{-1} and $\delta_{C\equiv C}$ 667 cm^{-1}) were shown in the FT-IR spectrum of GR/CS(UGT1A10)-PEG-C≡CH (curve b). After click reaction, the above azide and alkyne absorption peaks all disappeared in the curve c of Fig. S2, which indicated the generation of GR/CS(CYP1A2)-PEG- triazole-PEG-(UGT1A10)CS/GR and efficient performance of the click reaction.

Fig. S3

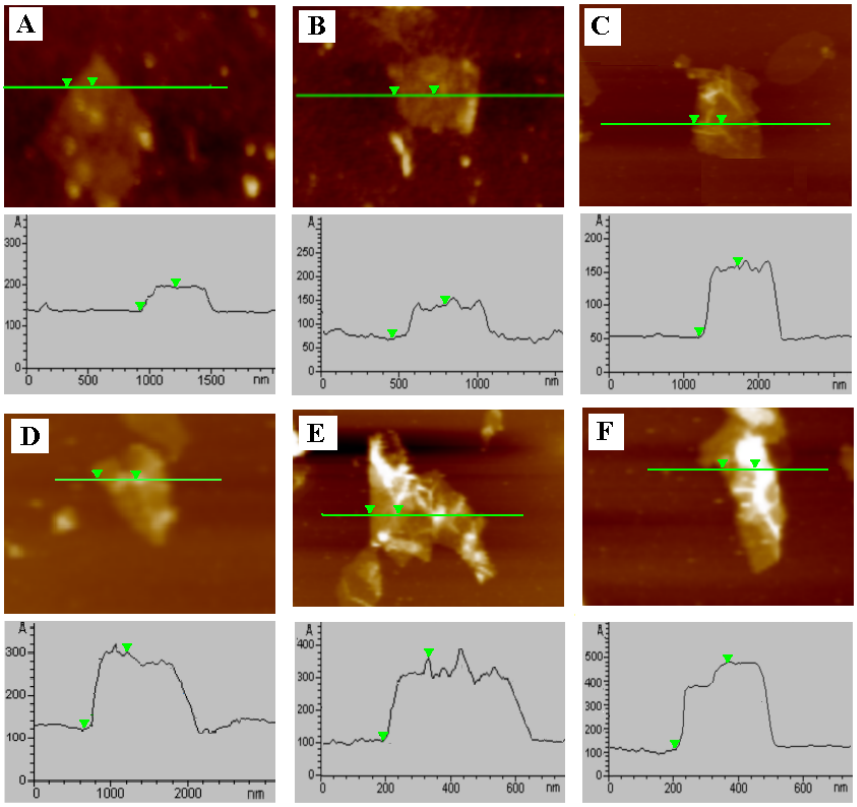

Fig. S3 AFM images and height profiles of graphene nano-cages linked with PEG of different chain lengths (molecular weights): (A) 550/550, (B) 550/1000, (C) 1000/1000, (D) 1000/2000, (E) 2000/2000, and (F) 2000/5000.

As shown in the AFM images (Fig. S3), when the molecular weights of the PEG in the upper and bottom layers of graphene nanosheets increase from 550/550, 550/1000, 1000/1000, 1000/2000, 2000/2000 to 2000/5000, the nano-cage outer-layer distance increases from about 6.5 nm, 8.0 nm, 11 nm, 20 nm, 28 nm to 40 nm accordingly. Thus, the present assembly strategy offers a practical way to construct multi-enzyme complexes in the nano-cage with controllable interlayer distance for studying the catalytic properties of cascade multi-enzymes.

Fig. S4

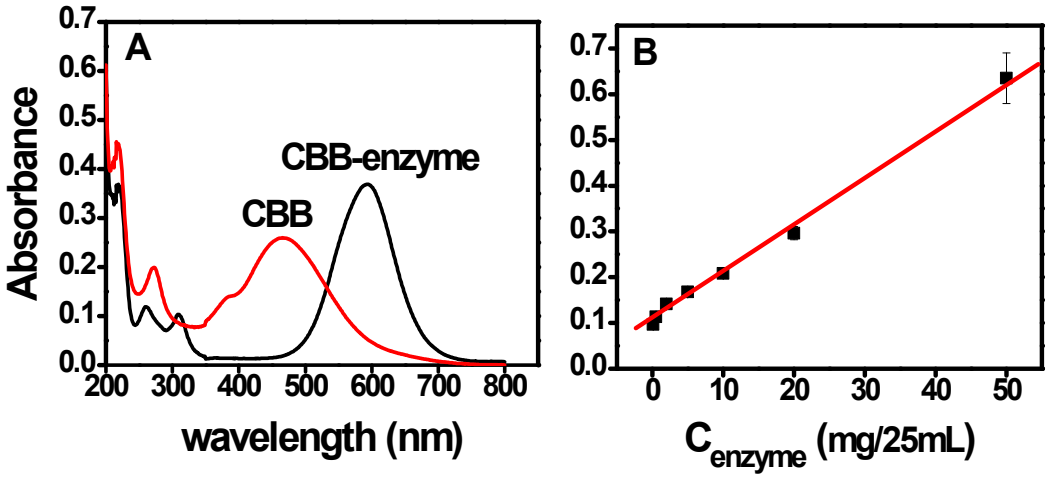

Fig. S4 (A) UV-vis spectra of Coomassie Brilliant Blue G-250 (CBB) and CBB-enzyme complex. (B) Plot of absorbance of CBB-enzyme and the concentration of enzyme in solution.

After immobilization on the GR/CS nanosheets, the amount of CYP1A2 or UGT1A10 remaining in the mixture solution was determined by the Bradford method. Briefly, 30 mL of the mixture solution added to 1 mL of Coomassie Brilliant Blue G-250 (0.1 g L^{-1} in water), and the optical density was measured at 595 nm after 30 min of incubation at room temperature using a UV-2450 spectrometer. The amount of enzyme in the solution was achieved according the calibration plot of Absorbance *versus* C_{enzyme} (Fig. S4). And the amount of CYP1A2 or UGT1A10 on the GR/CS nanosheets was obtained as the difference between total added amount of enzymes and the detected amount.

Fig. S5

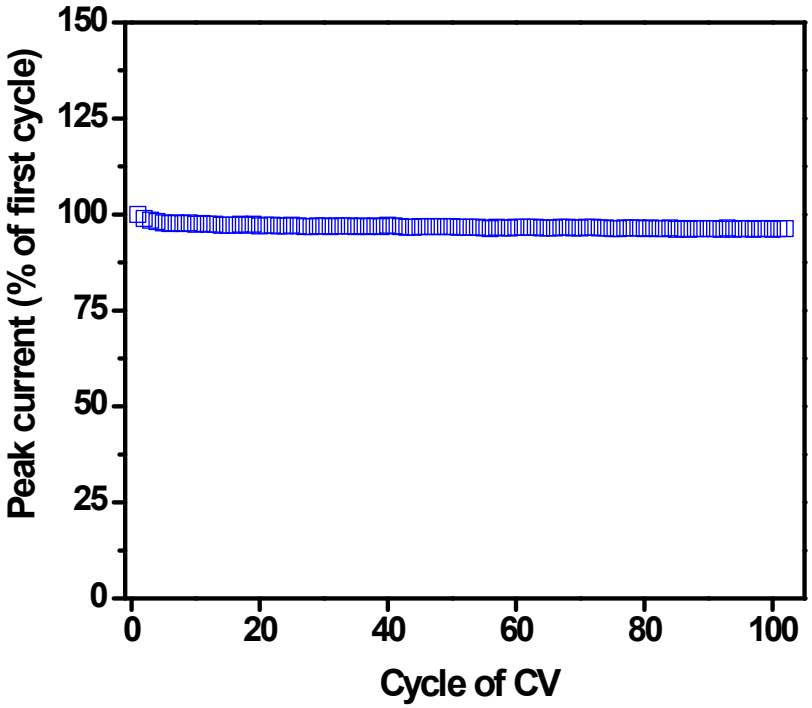

Fig. S5 Effect of scan cycles on the peak current of CYP1A2 in the graphene nano-cage. Electrolyte solution: anaerobic 0.1 M PBS (pH 7.4); Scan rate: 0.1 V s^{-1}.

To investigate the electrochemical characteristics of CYP1A2 in the graphene nano-cage, the effects of scan cycles on the CVs responses of immobilized CYP1A2 were studied. After more than 100 scan cycles, the peak current of CYP1A2 is essentially constant (Fig S5), which illustrates CYP1A2 on the modified GCE has good electrochemical stability.

Fig. S6

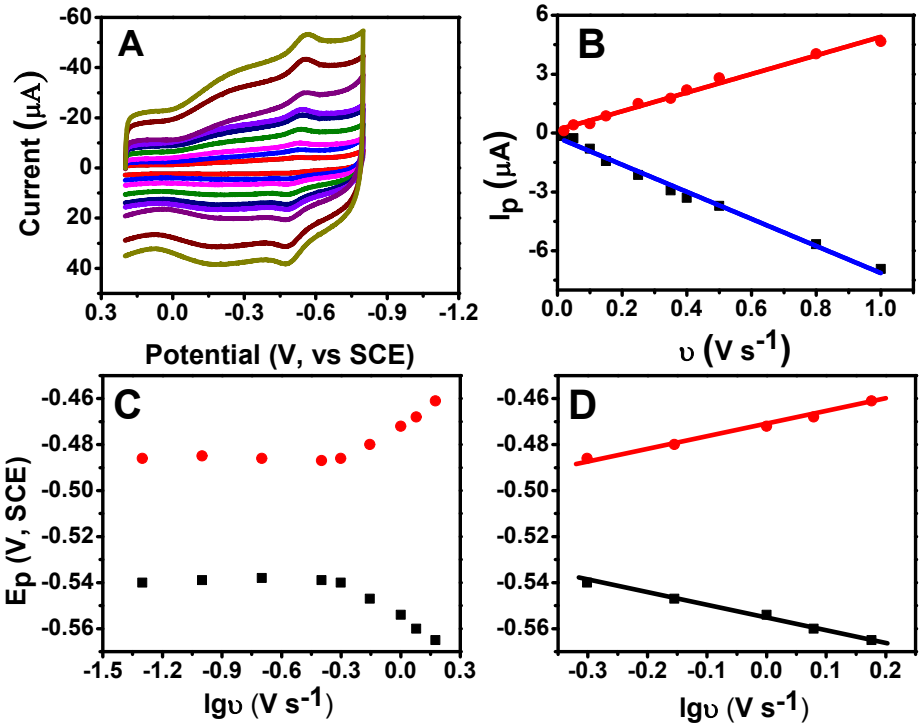

Fig. S6 (A) Cyclic voltammograms of **3** at different scan rates; (B) Plot of the peak current versus the scan rate (υ); (C, D) Plot of the peak potential versus log υ. Electrolyte solution: anaerobic 0.1 M PBS (pH 7.4); Range of scan rate: 0.05 to 1.5 V s^{-1}.

With the increase of scan rate from 0.05 to 1.5 V s^{-1}, the anodic and cathodic peak currents of CYP1A2 all increase (Fig. S6A), and the corresponding currents are proportional to the scan rate (Fig. S6B), indicating a typical of surface-controlled quasireversible process. Simultaneously, the anodic and cathodic peak potentials are linearly depended on the logarithm of scan rate (v) when the v was higher than 0.5 V s^{-1} (Fig. S6 C and D). Based on Laviron's equations,

$$E_{p,c} = E^{0'} - \frac{2.303RT}{\alpha nF} lg\upsilon \quad (1) \qquad E_{p,a} = E^{0'} + \frac{2.303RT}{(1-\alpha)nF} lg\upsilon \quad (2)$$

$$lgK_s = \alpha \lg(1-\alpha) + (1-\alpha)lg\alpha - lg\frac{RT}{nF\upsilon} - \frac{(1-\alpha)\alpha F\Delta E_p}{2.303RT} \quad (3)$$

The electron transfer coefficient (α) is calculated to be 0.496, so the heterogeneous electron transfer rate constant (K_s) is calculated to be 5.37 s^{-1} at the scan rate of 0.1 V s^{-1}, which indicated a fast electron transfer rate of CYP1A2 on the nano-cage modified GCE.

Fig. S7

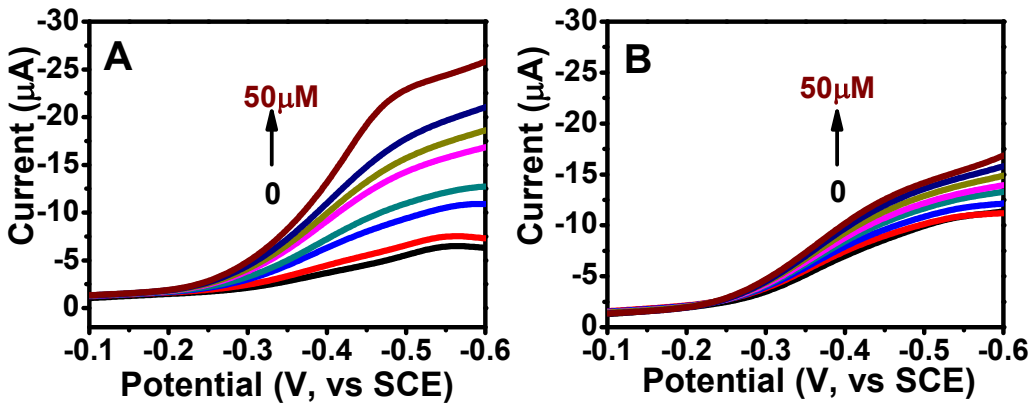

Fig. S7 Influence of warfarin concentration (0, 2, 4, 8, 15, 20, 40, 50 μM) on rotating disk voltammograms (1000 rpm) of enzymes in graphene nano-cage (A) or GCE/GR/CYP1A2& UGT1A10 (B). Electrolyte solution: aerobic 0.1 M PBS (pH 7.4); Scan rate: 0.1 V s^{-1}.

Fig. S8

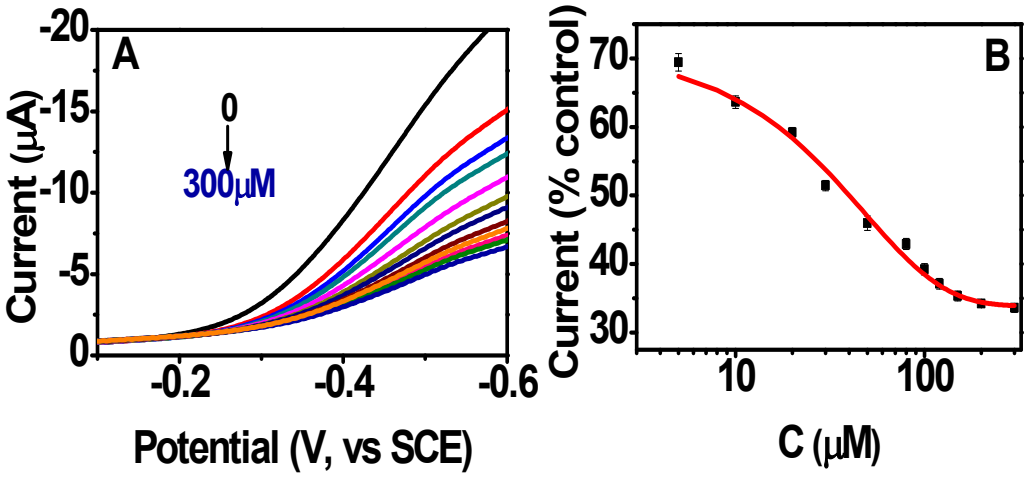

Fig. S8 Inhibition effect of ciprofloxacin on bioelectrocatalysis of enzymes in the graphene nano-cage. (A) Influence of ciprofloxacin concentration (0, 5, 10, 20, 30, 50, 80, 100, 120, 150, 200, 300 μM) on rotating disk voltammograms (1000 rpm) in aerobic 0.1 M PBS (pH 7.4) containing 100 μM warfarin at a scan rate of 0.1 V s^{-1}; (B) Change of the catalytic current of enzymes in the graphene nano-cage upon addition of ciprofloxacin. Molecular weight of the PEG chains in the upper and lower layer of graphene nano-cage: 2000 and 2000, respectively.

In which, the "current (% control)" is obtained by the catalytic current of enzymes (0 μM ciprofloxacin) divided by that at a certain concentration of ciprofloxacin (5, 10, 20, 30, 50, 80, 100, 120, 150, 200 or 300 μM).

Fig. S9

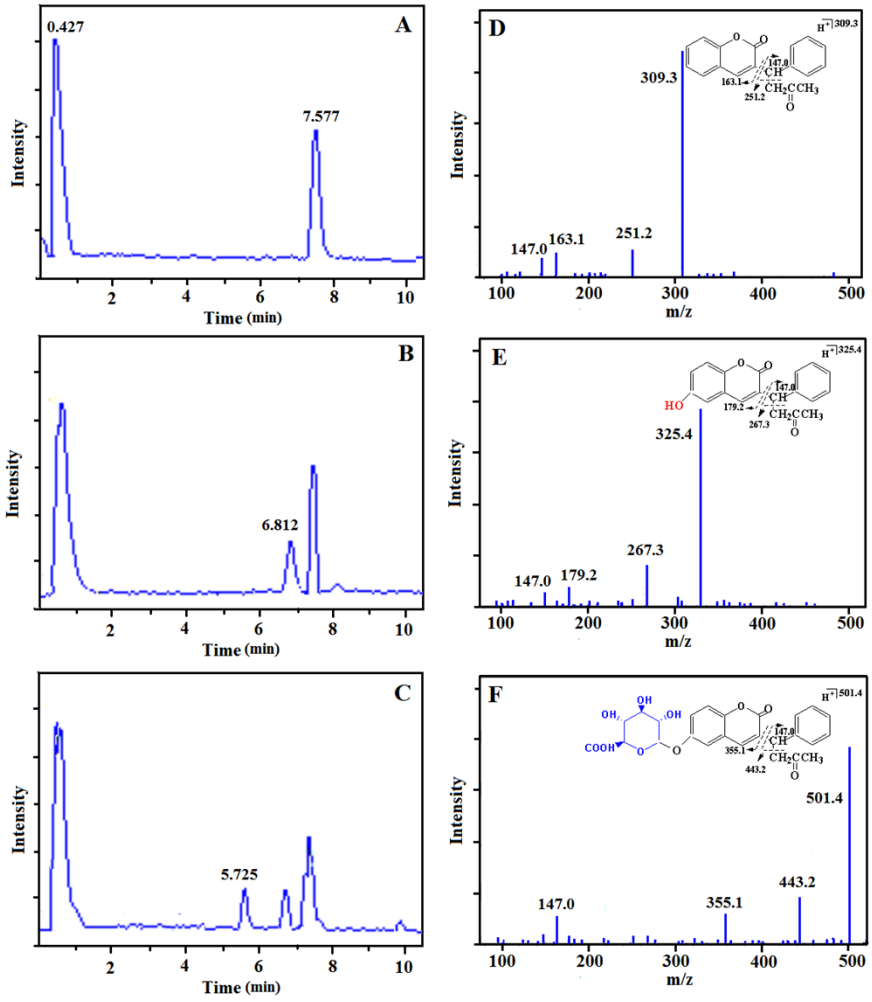

Fig. S9 Capillary HPLC-UV chromatograms (A-C) and mass spectra (D-F) of warfarin and its metabolites. HPLC chromatograms of warfarin (A), reaction mixture catalyzed by GCE/GR/CS/CYP1A2 (B) and reaction mixture catalyzed by CYP1A2/UGT1A10 bienzyme complexes in the nano-cage (C). Mass spectra of pure warfarin (D), phase I warfarin metabolite (E) and phase II warfarin metabolite (F). Electrolysis time and potential: 1 h and -0.54 V (vs SCE). Electrolyte solution: 0.1 M pH 7.4 PBS containing 100 μM warfarin, 2 mM UDPGA, 25 μg mL^{-1}alamethicin and 5 mM $MgCl_2$. Molecular weight of the PEG chains in the upper and bottom layer of nano-cage: 2000 and 2000, respectively. Insets show the ion peaks in the mass spectra, m/z 501.4, 325.4, and 309.3, as protonated molecular ions of 6-hydroxywarfarin glucuronide, 6-hydroxywarfarin warfarin, and warfarin, respectively.

References

S1 M. H. Huang, X. Xu, H. Yang and S. Q. Liu, *RSC Adv*., 2012, **2**, 12844.

S2 (a) Z. Y. Li and Y. Chau, *Polym. Chem.,* 2010, **1**, 1599; (b) S. Zalipsky, C. Gilon and A. Zilkha, *Eur. Polym. J.,* 1983, **19**, 1177.

S3 (a) X. M. Yang, Y. F. Tu, L. L. Li, S. M. Shang and X. M. Tao, *ACS Appl. Mater. Inter.,* 2010, **2**, 1707; (b) M. Li, Y. B. Wang, Q. Liu, Q. H. Li, Y. Cheng, Y. F. Zheng, T. F. Xi and S. C. Wei, *J. Mater. Chem. B,* 2013, **1**, 475.

S4 D. Li, M. B. Muller, S. Gilje, R. B. Kaner and G. G. Wallace, *Nat. Nanotechnol.,* 2008, **3**, 101.

S5 S. Villar-Rodil, J. I. Paredes, A. Martinez-Alonso and J. M. D. Tascon, *J. Mater. Chem.,* 2009, **19**, 3591.

S6 S. Stankovich, D. A. Dikin, R. D. Piner, K. A. Kohlhaas, A. Kleinhammes, Y. Y. Jia, Y. Wu, S. T. Nguyen and R. S. Ruoff, *Carbon,* 2007, **45**, 1558.

S7 J. Paredes, S. Villar-Rodil, P. Solis-Fernandez, A. Martinez-Alonso and J. Tascon, *Langmuir,*2009, **25**, 5957.

S8 (a) T. Kuila, S. Bose, A. K. Mishra, P. Khanra, N. H. Kim and J. H. Lee, *Prog. Mater. Sci.,* 2012, **57**, 1061; (b) P. Wu, Q. A. Shao, Y. J. Hu, J. A. Jin, Y. J. Yin, H. Zhang and C. X. Cai, *Electrochim. Acta,* 2010, **55**, 8606; (c) J. L. Zhang, H. J. Yang, G. X. Shen, P. Cheng, J. Y. Zhang and S. W. Guo, *Chem. Commun.,* 2010, **46**, 1112.